

the X-ray crystal structures of the sodium complexes of 2.2.1.²⁴ and 2.2.2.²⁵ it can be seen that in the 2.2.1. complex Na⁺ is unsymmetrically located in the cage with other oxygens at 249.1, 249.9, 245.1, 251.9, and 244.6 pm and in 2.2.2. on the other hand, Na⁺ is symmetrically surrounded by oxygen atoms, but distances are ca. 10 pm larger than in 2.2.1.

In both complexes the sodium ion at the center of an extended system possesses a large number of vibrational degrees of freedom which is further enhanced by the flexibility of the ligand. The fundamental bonding pattern is the same as in the solvate structure. The macrocyclic effect of the ligand does, however, lead to a higher degree of order, which opens up additional vibrational modes that are variable with regard to the ligand topology. Evidently then, macrocyclic polyethers are systems which are particularly sensitive to change in mass and which may even show resonance effects with masses of certain magnitudes. More specifically (1) in the Na⁺ complex of 2.2.1. the sum of the vibrational partition functions is larger than that of the solvate complex (accordingly (see Equilibrium Isotope Effects) enriched in the polyether complex), (2) the 2.2.2. complex with sodium shows longer lengths between Na⁺ and ether oxygens and thereby seriously alters the vibrational system so that compared with the solvate system the vibrational partition function is smaller and the lighter isotope preferentially bound), (3) attachment of nonrigid substituents, as, e.g., dodecyl groups, enhances ligand flexibility and the number of vibrational modes are increased for the cation, leading to decreased ²²Na enrichment, and (4) introduction of benzene rings into one or more ethylene bridges gives increased rigidity of the ligand and decreased cage volume.

As a consequence, the complex of Na⁺ with 2.2.2_B becomes more stable than that with 2.2.2. and bonding is more like that in the complex with 2.2.1.. On the other hand, the complex as a whole is more rigid due to incorporation of a benzene nucleus and its vibrational partition function is less than in Na⁺ 2.2.1.. However, the latter is larger than in the solvate complex, as shown by the ²⁴Na⁺ enrichment of 3.0 ± 0.4%. Further incorporation of benzene rings leads to more pronounced rigidity and there is

(24) Mathieu, F.; Metz, B.; Moras, D.; Christensen, J. J. *J. Am. Chem. Soc.* 1980, 102, 475.

(25) Mathieu, F.; Metz, B.; Moras, D.; Weiss, R. *J. Am. Chem. Soc.* 1978, 100, 4412.

no significant separation factor observed for 2.2_B, 2_B..

It is now possible to interpret the results found by Lee and Begun²⁶ for lithium isotopes on cation exchangers in which isotopic shifts depended on cross-linking of the exchanger, effects becoming larger with higher cross-linking. This can be explained by the different degrees of hydration of lithium cations on the exchanger which depends on the cross-linking. In the case of the hydrated systems more ordered structures can be formed, affecting the number of vibrational modes and the resultant partition function.

While these considerations allow qualitative predictions based on the work of Bigeleisen (eq 5) necessitate the exact analysis and characterization of the individual vibrational modes of the complexes. Further experimental work needs to be done to achieve this objective.

Even though these isotope effects involving sodium are only of interest in a theoretical context, their investigation is of more fundamental importance. Present methods of isotopic enrichment allow isotopes of sufficient purity to be obtained, but costs are very often prohibitive due to the smallness of the effects and the consequent expenditure of energy.

Chemical exchange methods are more economical, as, e.g., in the systems H₂O/HDS and HD/H₂O, respectively. However, these chemical systems have shown large isotope effects only in the case of exchange equilibria involving covalently bound nuclides. This is due to ion solvation, which it has not been possible to overcome without severe changes of bonding.

Macrocyclic polyethers now seem to offer the possibility of bonding interactions similar to those in the solvate complex while possessing a larger vibrational partition function that leads to equilibrium isotope effects and sufficiently fast kinetics of exchange, allowing the effects to be attained in finite time.

The use of macrocyclic polyethers or similar substances should therefore enable isotope enrichment by chemical exchange to be extended to ionic products.

Acknowledgment. This work has been supported by BMFT whose financial assistance is gratefully acknowledged. We also thank the GKSS for the opportunity to use their irradiation facilities at the nuclear reactor FRG 1.

(26) Moras, D.; Weiss, R. *Acta. Crystallogr., Sect. B* 1973, B29, 396.

(27) Lee, D. A.; Begun, G. M. *J. Am. Chem. Soc.* 1959, 81, 2332.

Microwave Spectrum and Unusual Geometry of Propadienone (Methylene Ketene)

Ronald D. Brown,* Peter D. Godfrey, Robert Champion, and Donald McNaughton

Contribution from the Department of Chemistry, Monash University, Clayton, Victoria 3168, Australia. Received March 12, 1981

Abstract: The microwave spectra of several isotopic species of propadienone, CH₂=C=C=O, have been analyzed to elucidate the geometry of this somewhat peculiar molecule. The heavy chain of atoms is found to be bent at the middle carbon by approximately 26° from the linear configuration. The nonlinearity is confirmed by the identification of cis and trans forms of monodeuteriopropadienone, by the lack of intensity alternation in the spectral lines, and by a substantial perpendicular component of the dipole moment [$\mu_b = 0.7914$ (6) D; $\mu_a = 2.156$ (3) D; $\mu_{\text{total}} = 2.297$ (3) D]. Both the geometry and the dipole moment are at variance with recent results of elaborate molecular orbital calculations.

The microwave spectrum of propadienone (H₂C₃O) was first observed in these laboratories as a means of demonstrating unambiguously the generation of the compound by flash vacuum pyrolysis.¹ The analysis of the spectra of H₂C₃O, HDC₃O, and D₂C₃O implied that the molecule was probably planar.² However

(1) G. L. Blackman, R. D. Brown, R. F. C. Brown, F. W. Eastwood, G. L. McMullen, and M. L. Robertson, *Aust. J. Chem.*, 31, 209 (1978).

the moments of inertia suggested the presence of in-plane distortion or large-amplitude vibration and that the molecule is not a simple relative of formaldehyde and ketene. This structural uncertainty has been resolved from a more extensive study of the rotational spectra of some isotopic species of propadienone. We present here

(2) G. L. Blackman, R. D. Brown, R. F. C. Brown, F. W. Eastwood, and G. L. McMullen, *J. Mol. Spectrosc.*, 68, 488 (1977).

results which show unambiguously that the molecule has C_s and not C_{2v} symmetry and offer a relatively simple explanation of its geometry. Our results however are in conflict with elaborate molecular orbital studies of the molecular geometry.^{3,4} (Dunning-contracted triple- ζ plus polarization basis set—ref 4.)

Experimental Section

The various isotopic species of propadienone were generated by flash vacuum pyrolysis of the appropriate isotopic versions of acrylic anhydride. Acrylic anhydride was prepared by acylation of acrylic acid with acryloyl chloride.⁵

Monodeuterioacrylic acid (HDC=CH—COOH) was prepared by deuteration of propionic acid⁶ followed by hydrogenation and collection as the sodium salt. The ¹⁸O-labeled acrylic acid was prepared by exchange with H₂¹⁸O. The spectrum of the ¹³C species (¹³CH₂=C=C=O) was observed in natural abundance.

The microwave spectrometer was a standard 5-kHz Stark-modulated instrument having a 3-m long G-band cell with the sample inlet tube from the pyrolysis oven at one end and a liquid-nitrogen trap at the other. A gas-stream inlet pressure of around 0.25 Pa was used. The microwave sources were either a Hewlett-Packard KO3-8690A phase-locked backward wave oscillator or a suitable OKI klystron phase locked to an appropriate reference oscillator. Lines were usually repetitively scanned, the spectral data being accumulated and reduced in a Varian V75 computer system. The frequency scale was established with a Hewlett-Packard 5246L counter, periodically calibrated against a Sulzer 2.5c laboratory frequency standard and the Australian national frequency standard transmitted by VNG Lyndhurst.

Center frequencies of spectral lines were mostly determined by a least-squares fitting of a Lorentzian curve to an appropriate section of the spectrometer's digitized and averaged output. The location of center frequencies was typically reproducible to about 5 kHz. We believe that systematic errors associated with line frequencies would be less than 5 kHz. In general, standard deviations for line frequencies were estimated as one-tenth of the line width (fwhm). Line widths were generally between 60 and 200 kHz.

Determination of relative frequencies of lines for Stark effect measurements, again made by line-shape fitting procedures, showed standard deviations from the relevant Stark effect formulas of the same magnitude as estimated measurement errors.

The electric field calibration for the Stark-effect measurements was based on measurements on OCS for which the electric dipole moment was taken to be 0.71521 D.⁷

Results

The spectrum of propadienone shows characteristics of a near-symmetric prolate top having C_s symmetry. The low- J , ^aR-branch lines have been assigned for the species H₂C₃O, ¹³CH₂=C=C=O, H₂C₃¹⁸O, *cis*-HDC₃O, *trans*-HDC₃O, and D₂C₃O. The $K_a = 1$, ^qQ-branch lines for $J = 8-23$ and ten ^bP- and ^bR-branch lines have been assigned for the abundant species.

Moderately large centrifugal distortion contributions to the frequencies are evident, requiring the inclusion in the Hamiltonian of terms up to the eighth power in angular momentum. Satisfactory agreement was achieved (i.e., no statistically significant improvement in the least-squares fitting was obtainable by adding still higher order terms to the Hamiltonian) between calculated and observed spectral line frequencies.

The S -reduced Hamiltonian^{8,9} was used in a weighted least-squares fit of the observed frequencies.

$$\begin{aligned} \tilde{H} = & \frac{1}{2}(B + C)\tilde{J}^2 + (A - \frac{1}{2}(B + C))\tilde{J}_a^2 + \\ & \frac{1}{4}(B - C)(\tilde{J}_+^2 + \tilde{J}_-^2) - D_J\tilde{J}^4 - \\ & D_{JK}\tilde{J}^2\tilde{J}_a^2 - D_K\tilde{J}_a^4 + d_1\tilde{J}^2(\tilde{J}_+^2 + \tilde{J}_-^2) + d_2(\tilde{J}_+^4 + \tilde{J}_-^4) + \\ & H_J\tilde{J}^6 + H_{JK}\tilde{J}^4\tilde{J}_a^2 + H_{KJ}\tilde{J}^2\tilde{J}_a^4 + H_K\tilde{J}_a^6 + \\ & h_1\tilde{J}_+^4(\tilde{J}_+^2 + \tilde{J}_-^2) + h_2\tilde{J}_-^4(\tilde{J}_+^2 + \tilde{J}_-^2) + h_3(\tilde{J}_+^6 + \tilde{J}_-^6) + \\ & I_{JKK}\tilde{J}^2\tilde{J}_a^6 \end{aligned}$$

(3) L. Radom, *Aust. J. Chem.*, **31**, 1 (1978).

(4) A. Komonnicki, C. E. Dykstra, M. A. Vincent, and L. Radom, *J. Am. Chem. Soc.*, **103**, 1652 (1981).

(5) T. K. Brotherton, J. Smith, Jr., and J. W. Lynn, *J. Org. Chem.*, **26**, 1283 (1961).

(6) R. K. Hill and G. R. Newkome, *J. Org. Chem.*, **34**, 740 (1969).

(7) J. S. Muenter, *J. Chem. Phys.*, **48**, 4544 (1968).

(8) B. P. Van Eijck, *J. Mol. Spectrosc.*, **53**, 246 (1974).

(9) J. K. G. Watson in "Vibrational Spectra and Structure", Vol. 6, J. R. Durig, Ed., Elsevier, Amsterdam, 1978, Chapter 1.

The results of the analyses are presented in Tables I and II. Stark shift measurements were made on four transitions: $2_{12}^-1_{11}$, $8_{1,7}^-8_{1,8}$, $9_{1,8}^-9_{1,9}$, and $15_{1,14}^-15_{1,15}$. The dipole moment components were determined from a least-squares fit on 32 measurements in all.

$$\mu_a = 2.156 \text{ (3) D}$$

$$\mu_b = 0.7914 \text{ (6) D}$$

The $15_{1,14}^-15_{1,15}$ transition shows the effect of a b -type near degeneracy of 111.69 MHz between the $16_{0,16}$ and $15_{1,15}$ energy levels. The first-order nature of the resulting Stark effect enabled accurate predictions of b -type transitions to be made. Further discussion of this point is made below.

Measurements on the $17_{1,16}^-17_{1,17}$ transition, involving a c -type near degeneracy, enabled us to place and upper limit on μ_c of 0.05 D.

Discussion

Relative Intensities. Relative intensity measurements were made on a number of a -type transitions of propadienone to determine whether the 3:1 statistical weighting for K_a -odd and K_a -even energy levels, consistent with C_{2v} symmetry, is observed.

The Stark-cell spectrometer used was not designed to achieve accuracy in such measurements. To test the validity of conclusions arrived at from relative intensity measurements, we investigated a number of transitions of *o*-difluorobenzene. These included ground-state and vibrational satellite lines. Errors were found to be no greater than 20%.

The results of measurements on propadienone are presented in Table III. It is apparent that the 3:1 statistical weighting is not observed and the relative intensities are consistent with a structure having C_s symmetry.

This hypothesis was verified by the detection of the μ_b component of the dipole moment and the presence of the b -type spectrum and the assignment of the spectrum of two singly deuterated species.

Determination of A from Near-Degenerate Stark Effect. In most cases, the initial assignment of the rotational spectrum of near-symmetric prolate tops is the a -type spectrum. Often, the A rotational constant determined from these transitions has a large uncertainty because the dependence on A is second order. Hence b -type transitions (which have frequencies dependent on an AK_a^2 term) are poorly predicted.

The b -type Stark effect in a -type transitions is dependent on this same AK_a^2 term and is very sensitive to the value of A when near degeneracies (such as we have reported above) occur.¹⁰

The near degeneracies, useful in the present context, occur between levels of the form $J_{0,J}$ and $(J-1)_{1,J-1}$. When asymmetry doubling and centrifugal distortion effects are neglected, the associated energy gap may be approximately expressed as

$$\Delta E_{ij} \approx \pm[(B + C)J - (A - \frac{1}{2}B - \frac{1}{2}C)]$$

Hence near degeneracies occur when

$$J \approx A/(B + C) - \frac{1}{2}$$

for all near-symmetric prolate tops. For propadienone this gives $J \approx 16$.

The energy levels, when a perturbing electric field is applied, may be expressed as

$$E_i = E_i^0 + \sum_j \epsilon^2 \mu_{ij}^2 / \Delta E_{ij} \quad (1)$$

provided that $|\Delta E_{ij}| \gg |\epsilon \mu_{ij}|$, where E_i^0 is the unperturbed energy, ϵ is the electric field, $\Delta E_{ij} = E_i^0 - E_j^0$, and μ_{ij} is the appropriate dipole moment matrix element.

(10) R. D. Brown and P. D. Godfrey, to be submitted for publication.

Table 1^bA. Rotational Transition Frequencies (MHz) of Propadienone (CH₂=C=C=O)

rotational transition	obsd freq	obsd - calcd freq	rotational transition	obsd freq	obsd - calcd freq
8 _{1,7} -8 _{1,8}	4 639.233 (16)	0.006	12 _{1,12} -13 _{0,13}	28 330.265 (8)	-0.001
9 _{1,8} -9 _{1,9}	5 798.286 (15)	0.005	19 _{0,19} -18 _{1,18}	29 026.882 (8)	0.001
11 _{1,10} -11 _{1,11}	8 501.557 (5)	-0.001	21 _{1,20} -21 _{1,21}	29 681.714 (11)	-0.001
1 ₀₁ -0 ₀₀	8 645.159 (8) ^a	0.007	22 _{1,21} -22 _{1,22}	32 497.417 (10)	0.008
14 _{1,14} -15 _{0,15}	9 423.100 (8)	-0.001	4 ₁₄ -3 ₁₃	34 328.545 (14) ^a	0.004
17 _{0,17} -16 _{1,16}	9 699.096 (9)	-0.003	4 ₀₄ -3 ₀₃	34 579.377 (8) ^a	-0.001
12 _{1,11} -12 _{1,12}	10 045.533 (6)	-0.003	4 ₂₃ -3 ₂₂	34 604.950 (25) ^a	-0.016
13 _{1,12} -13 _{1,13}	11 717.555 (5)	-0.001	4 ₂₂ -3 ₂₁	34 605.784 (25) ^a	-0.022
14 _{1,13} -14 _{1,14}	13 517.464 (7)	-0.002	4 ₃₂ -3 ₃₁	} 34 634.945 (25) ^a	0.006
15 _{1,14} -15 _{1,15}	15 445.100 (7)	0.004	4 ₃₁ -3 ₃₀		
2 ₁₂ -1 ₁₁	17 164.485 (10) ^a	0.001	4 ₁₃ -3 ₁₂	34 844.164 (17) ^a	0.006
2 ₀₂ -1 ₀₁	17 290.179 (6) ^a	-0.002	23 _{1,22} -23 _{1,23}	35 438.921 (9)	-0.001
2 ₁₁ -1 ₁₀	17 422.331 (7) ^a	-0.005	11 _{1,11} -12 _{0,12}	37 700.543 (8)	0.001
16 _{1,15} -16 _{1,16}	17 500.272 (7)	0.008	20 _{0,20} -19 _{1,19}	38 764.635 (9)	0.001
13 _{1,13} -14 _{0,14}	18 904.126 (9)	0.012	5 ₁₅ -4 ₁₄	42 910.281 (11)	0.004
18 _{0,18} -17 _{1,17}	19 337.932 (9)	0.009	5 ₀₅ -4 ₀₄	43 223.302 (14)	0.002
18 _{1,17} -18 _{1,18}	21 992.410 (7)	0.002	5 ₃₃ -4 ₃₂	} 43 293.479 (25)	0.005
19 _{1,18} -19 _{1,19}	24 428.935 (8)	-0.008	5 ₃₂ -4 ₃₁		
3 ₁₃ -2 ₁₂	25 746.591 (8) ^a	-0.001	5 ₄₂ -4 ₄₁	} 43 342.947 (25)	-0.001
3 ₀₃ -2 ₀₂	25 934.968 (7) ^a	0.004	5 ₄₁ -4 ₄₀		
3 ₂₂ -2 ₂₁	25 953.893 (25) ^a	-0.010	5 ₁₄ -4 ₁₃	43 554.718 (10)	0.003
3 ₂₁ -2 ₂₀	25 954.245 (25) ^a	0.006	10 _{1,10} -11 _{0,11}	47 013.970 (15)	-0.021
3 ₁₂ -2 ₁₁	26 133.341 (7) ^a	-0.003	21 _{0,21} -20 _{1,20}	48 549.776 (10)	-0.003
20 _{1,19} -20 _{1,20}	26 992.129 (7)	-0.003			

B. Rotational Transition Frequencies (MHz) of Substituted Propadienone

<i>cis</i> -CHD=C=C=O			<i>trans</i> -CHD=C=C=O		
rotational transition	obsd freq	obsd - calcd freq	rotational transition	obsd freq	obsd - calcd freq
1 ₀₁ -0 ₀₀	8 287.130 (50)	-0.027	1 ₀₁ -0 ₀₀	8 125.844 (44)	-0.002
2 ₁₂ -1 ₁₁	16 407.381 (50)	-0.007	2 ₁₂ -1 ₁₁	16 129.626 (50)	-0.045
2 ₀₂ -1 ₀₁	16 574.037 (50)	-0.025	2 ₀₂ -1 ₀₁	16 251.545 (50)	-0.030
2 ₁₁ -1 ₁₀	16 744.810 (50)	-0.041	2 ₁₁ -1 ₁₀	16 377.013 (50)	-0.057
3 ₁₃ -2 ₁₂	24 610.826 (15)	-0.010	3 ₁₃ -2 ₁₂	24 194.364 (14)	-0.003
3 ₀₃ -2 ₀₂	24 860.464 (16)	0.002	3 ₀₃ -2 ₀₂	24 377.060 (14)	-0.006
3 ₂₂ -2 ₂₁	24 872.300 (50)	0.010	3 ₂₂ -2 ₂₁	24 387.637 (13)	0.005
3 ₂₁ -2 ₂₀	24 873.224 (50)	0.113	3 ₂₁ -2 ₂₀	24 387.960 (80)	-0.006
3 ₁₂ -2 ₁₁	25 117.038 (17)	0.009	3 ₁₂ -2 ₁₁	24 565.493 (19)	0.027
4 ₁₄ -3 ₁₃	32 813.998 (23)	0.010	4 ₁₄ -3 ₁₃	32 258.938 (30)	0.040
4 ₀₄ -3 ₀₃	33 146.122 (28)	0.018	4 ₀₄ -3 ₀₃	32 502.202 (26)	-0.001
4 ₂₃ -3 ₂₂	33 162.661 (20)	-0.011	4 ₂₃ -3 ₂₂	32 516.606 (17)	-0.009
4 ₂₂ -3 ₂₁	33 164.726 (33)	0.003	4 ₂₂ -3 ₂₁	32 517.452 (17)	-0.003
4 ₃₂ -3 ₃₁	} 33 181.055 (27)	-0.002	4 ₃₂ -3 ₃₁	} 32 533.713 (50)	0.008
4 ₃₁ -3 ₃₀					
4 ₁₃ -3 ₁₂	33 488.893 (24)	-0.018	4 ₁₃ -3 ₁₂	32 753.679 (28)	-0.017

¹³ CH ₂ =C=C=O			CH ₂ =C=C= ¹⁸ O		
rotational transition	obsd freq	obsd - calcd freq	rotational transition	freq	obsd - calcd freq
2 ₁₂ -1 ₁₁	16 659.450 (100)	0.088	1 ₀₁ -0 ₀₀	8 218.761 (23)	0.021
2 ₀₂ -1 ₀₁	16 778.481 (29)	0.005	2 ₁₂ -1 ₁₁	16 323.534 (14)	-0.018
3 ₁₃ -2 ₁₂	24 988.928 (25)	-0.005	2 ₀₂ -1 ₀₁	16 437.421 (25)	0.040
3 ₀₃ -2 ₀₂	25 167.460 (14)	0.002	2 ₁₁ -1 ₁₀	16 557.306 (13)	0.022
3 ₂₂ -2 ₂₁	25 186.020 (100)	-0.020	3 ₁₃ -2 ₁₂	24 485.180 (10)	-0.020
3 ₂₁ -2 ₂₀	25 186.320 (100)	-0.030	3 ₀₃ -2 ₀₂	24 655.858 (25)	0.033
3 ₁₂ -2 ₁₁	25 355.570 (100)	-0.143	3 ₂₂ -2 ₂₁	24 673.639 (50)	-0.051
4 ₁₄ -3 ₁₃	33 318.369 (20)	-0.002	3 ₂₁ -2 ₂₀	24 673.868 (50)	-0.077
4 ₂₃ -3 ₂₂	33 581.214 (20)	0.002	3 ₁₂ -2 ₁₁	24 835.835 (20)	0.037
4 ₂₂ -3 ₂₁	33 581.991 (20)	0.002	5 ₁₅ -4 ₁₄	40 808.013 (13)	0.023
4 ₃₂ -3 ₃₁	} 33 611.182 (65)	-0.002	5 ₀₅ -4 ₀₄	41 091.726 (13)	-0.001
4 ₃₁ -3 ₃₀					
4 ₁₃ -3 ₁₂	33 807.440 (100)	0.027	5 ₂₄ -4 ₂₃	41 122.119 (100)	-0.091
			5 ₂₃ -4 ₂₂	41 123.503 (100)	0.021
			5 ₃₃ -4 ₃₂	} 41 157.846 (16)	0.010
			5 ₃₂ -4 ₃₁		
			5 ₄₂ -4 ₄₁	} 41 204.472 (11)	-0.001
			5 ₄₁ -4 ₄₀		
			5 ₁₄ -4 ₁₃	41 392.302 (11)	-0.016

^a Remeasurements of previously assigned lines. ^b Errors quoted are estimated standard deviations for frequency measurements.

Table II^a

A. Rotational and Distortion Constants (MHz) for Propadienone					
parameter	CH ₂ C=C=O	<i>cis</i> -CHDC=C=O	<i>trans</i> -CHDC=C=O	¹³ CH ₂ =C=C=O	CH ₂ =C=C= ¹⁸ O
<i>A-D_K</i> ^b	149 830.319 (24)	108 238 (1580)	140 756 (2891)	148 421 (3482)	165 076 (5024)
<i>B</i>	4387.045 99 (46)	4227.9482 (46)	4124.7758 (44)	4255.7767 (46)	4167.8057 (41)
<i>C</i>	4258.112 29 (46)	4059.2171 (44)	4001.0764 (38)	4133.5165 (60)	4050.9399 (34)
<i>D_J</i>	0.001 555 8 (58)	0.001 98 (16)	0.001 43 (11)	0.001 02 (18)	0.001 457 (78)
<i>D_{JK}</i>	-0.789 67 (42)	-0.4646 (18)	-0.4283 (12)	-0.7690 (16)	-0.7464 (11)
<i>d</i> ₁	-0.000 228 662 (97)				
<i>d</i> ₂	-0.000 034 0 (24)				
<i>H_J</i>	-0.000 000 053 3 (33)				
<i>H_{KJ}</i>	-0.003 872 (84)	-0.001 48 (18)	-0.000 53 (16)	-0.001 93 (16)	-0.003 163 (59)
<i>I_{JKKK}</i>	0.000 032 0 (39)				
Δ ^c	0.1151 (2)				

B. Correlation Matrices for Parameters H ₂ C ₃ O										
	<i>A</i>	<i>B</i>	<i>C</i>	<i>D_J</i>	<i>D_{JK}</i>	<i>d</i> ₁	<i>d</i> ₂	<i>H_J</i>	<i>H_{KJ}</i>	<i>I_{JKKK}</i>
<i>A</i>	1.00	0.84	0.84	0.82	0.91	-0.06	-0.05	0.59	0.78	-0.68
<i>B</i>		1.00	0.99	0.86	0.83	-0.05	-0.05	0.78	0.68	-0.59
<i>C</i>			1.00	0.87	0.83	0.08	0.08	0.78	0.68	-0.59
<i>D_J</i>				1.00	0.96	0.03	0.03	0.94	0.84	-0.74
<i>D_{JK}</i>					1.00	0.00	0.00	0.82	0.91	-0.82
<i>d</i> ₁						1.00	0.99	0.04	0.00	-0.00
<i>d</i> ₂							1.00	0.04	0.00	-0.00
<i>H_J</i>								1.00	0.72	-0.63
<i>H_{KJ}</i>									1.00	-0.98
<i>I_{JKKK}</i>										1.00

<i>cis</i> -HDC ₃ O						<i>trans</i> -HDC ₃ O							
	<i>A</i>	<i>B</i>	<i>C</i>	<i>D_J</i>	<i>D_{JK}</i>	<i>H_{KJ}</i>		<i>A</i>	<i>B</i>	<i>C</i>	<i>D_J</i>	<i>D_{JK}</i>	<i>H_{KJ}</i>
<i>A</i>	1.00	-0.15	-0.14	0.40	-0.74	-0.63	<i>A</i>	1.00	-0.33	-0.31	-0.04	-0.62	-0.42
<i>B</i>		1.00	0.28	0.59	0.12	0.15	<i>B</i>		1.00	0.12	0.63	0.30	0.25
<i>C</i>			1.00	0.59	0.12	0.15	<i>C</i>			1.00	0.58	0.29	0.27
<i>D_J</i>				1.00	-0.49	-0.38	<i>D_J</i>				1.00	-0.12	-0.01
<i>D_{JK}</i>					1.00	0.96	<i>D_{JK}</i>					1.00	0.90
<i>H_{KJ}</i>						1.00	<i>H_{KJ}</i>						1.00

¹³ CH ₂ =C=C=O						CH ₂ =C=C= ¹⁸ O							
	<i>A</i>	<i>B</i>	<i>C</i>	<i>D_J</i>	<i>D_{JK}</i>	<i>H_{KJ}</i>		<i>A</i>	<i>B</i>	<i>C</i>	<i>D_J</i>	<i>D_{JK}</i>	<i>H_{KJ}</i>
<i>A</i>	1.00	-0.23	-0.10	0.11	-0.59	-0.51	<i>A</i>	1.00	-0.02	-0.12	0.55	-0.70	-0.61
<i>B</i>		1.00	-0.08	0.26	0.12	0.05	<i>B</i>		1.00	0.20	0.63	0.12	0.14
<i>C</i>			1.00	0.85	-0.41	-0.28	<i>C</i>			1.00	0.46	0.22	0.22
<i>D_J</i>				1.00	-0.67	-0.52	<i>D_J</i>				1.00	-0.42	-0.34
<i>D_{JK}</i>					1.00	0.93	<i>D_{JK}</i>					1.00	0.98
<i>H_{KJ}</i>						1.00	<i>H_{KJ}</i>						1.00

^a Errors quoted are one standard deviation from least-squares fit. ^b The *A* rotational constants require qualification. For the main species *D_K* is expected to be of the order of 10 MHz. For the substituted species errors of up to 10% may be expected, related to the distortion parameter *d*₂. Correlation problems prevent *d*₂ from being adjusted in the fit. This uncertainty causes inertial defect values to be meaningless; hence they are not given. ^c Uncertainty in inertial defect allows for 10 MHz uncertainty in *A*. Δ is quoted in units of uÅ².

Table III

<i>K_a</i> = 1	<i>K_a</i> = 0	relative intensities (<i>I_{K=1}</i> / <i>I_{K=0}</i>)		
		<i>C</i> _{2v}	<i>C_s</i>	obsd
2 ₁₂ -1 ₁₁	} 2 ₀₂ -1 ₀₁	2.28	0.76	0.65
2 ₁₁ -1 ₁₀		2.34	0.78	0.62
4 ₁₄ -3 ₁₃	} 4 ₀₄ -3 ₀₃	2.84	0.95	0.89
4 ₁₃ -3 ₁₂		2.92	0.97	0.88

A near degeneracy is treated separately by finding the appropriate root of the 2 × 2 secular determinant. Hence the 15_{1,15} energy level, in the Stark shift calculations described, has the form

$$E = E^0 - \frac{\Delta E_{ik}}{2} + \left[\frac{(\Delta E_{ik})^2}{2} + \epsilon^2 \mu_{ik}^2 \right]^{1/2} + \sum_{j \neq k} \frac{\epsilon^2 \mu_{ij}^2}{\Delta E_{ij}} \quad (2)$$

where $\Delta E_{ik} = E_{15,15}^0 - E_{16,16}^0$.

Two cases require consideration. When ΔE_{ik} is sufficiently small (as we observed for propadienone), requiring the two-level formula (eq 2) to be used, measurement of the Stark effect of

Table IV. Cumulenone Dipole Moments (D)

formaldehyde ¹⁵	2.3321 (5)	propadienone	2.297 (3)
ketene ¹⁵	1.422 15 ^a	butatrienone	1.967 (3) ^b

^a No uncertainty reported. ^b Since previous publication,¹⁶ a more thorough statistical analysis has reduced the uncertainty significantly.

just one appropriate *a*-type transition at different field strengths enables both μ_b and *A* to be determined simultaneously.

Using this procedure, we determined *A* with an uncertainty of 2 MHz and found the *b*-type transitions within 5 MHz of their predicted frequencies. It is worth noting that the uncertainty in *A* from analysis of the *a*-type spectrum alone was ~1 GHz.

Alternatively, if the second-order formula 1 is applicable for ΔE_{ik} also, then measurement of the Stark effect for two *a*-type transitions (involving different ΔE_{ij}) enables μ_b and *A* to be determined simultaneously.

We present a revised list of dipole moments of the cumulenone series of molecules in Table IV. The alternating magnitude of these dipole moments has been discussed before.³ The revised value for propadienone does not contradict the qualitative arguments used to explain this alternation. However, the calculated

dipole moment^{3,4} remains at odds with the experimentally determined value. Indeed, the contribution of the resonance form IV, advanced to explain the structure of propadienone, may also explain the smaller dipole moment.

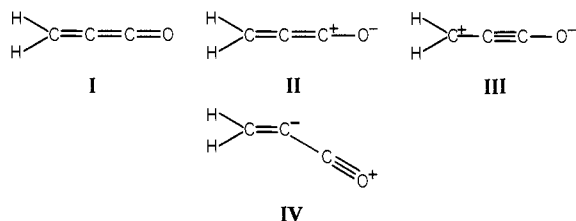
The Structure. From the small value of the inertial defect and also from the very small upper limit to the magnitude of μ_c , we can deduce that propadienone is planar.

The substitution data presented are insufficient for derivation of a complete r_s structure. Because the A rotational constants are not accurately determined, Kraitchman's equations do not provide accurate values of coordinates perpendicular to the a axis. The structure has been determined from a least-squares fit on the B and C rotational constants, subject to two constraints. Firstly, rigid planarity is assumed and secondly the $C=C=O$ angle is fixed at 180° .

The rigid planarity constraint introduces errors related to the inertial defect. These errors, in the main, affect the methylene group geometry. For comparison we present structures for formaldehyde¹¹ and ketene,¹² calculated in an identical fashion; i.e., literature frequencies were fitted by using the S -reduced Hamiltonian and the values of B and C obtained were used in a least-squares fit to determine the structures. These, with the reported structures, are presented in Figure 1.

The fixing of the $C=C=O$ angle at 180° is somewhat arbitrary. However, least-squares fits, fixing the methylene group angles between 115° and 120° and allowing the remaining structural parameters to vary, indicate that the $C=C=O$ angle cannot be more than 7° on either side of the linear configuration. This uncertainty could be resolved by analysis of the spectrum for the remaining ^{13}C isotopic species, but this presents considerable experimental problems.

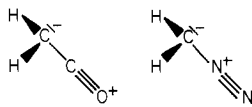
The somewhat unexpected structure of propadienone can nevertheless be understood in terms of a simple argument based on resonance structures. The structure may be considered as being a combination of the forms I-IV.



The contribution of III has been considered in relation to the dipole moment.³ The contribution of IV tends to produce a bend in the heavy-atom chain at C(2) because of the lone pair on this carbon. It appears that it is this contributing structure that is primarily responsible for the unexpected geometry of propadienone.

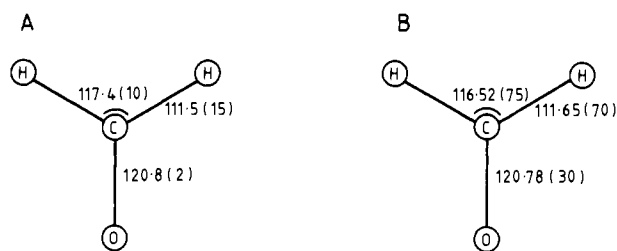
The contribution of a similar structure has been put forward to explain abnormally low force constants associated with methylene wagging vibrations of ketene¹³ and diazomethane.¹⁴

These are

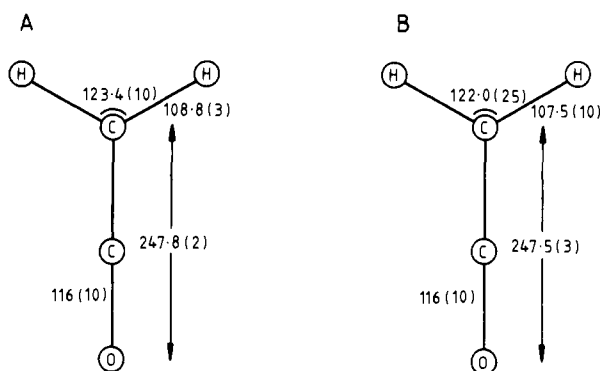


- (11) K. Takagi and T. Oka, *J. Phys. Soc. Jpn.*, **18** (8), 1174 (1963).
 (12) H. R. Johnson and M. W. P. Strandberg, *J. Chem. Phys.*, **20** (4), 687, (1952).
 (13) C. B. Moore and G. C. Pimentel, *J. Chem. Phys.*, **38** (12), 2816, (1963).
 (14) C. B. Moore and G. C. Pimentel, *J. Chem. Phys.*, **40** (2), 342, (1964).
 (15) B. Fabricant, D. Kreiger, and J. S. Muentner, *J. Chem. Phys.*, **67** (4), 1576 (1977).
 (16) R. D. Brown, R. F. C. Brown, F. W. Eastwood, P. D. Godfrey and D. McNaughton, *J. Am. Chem. Soc.*, **101**, 4705 (1979).

Formaldehyde



Ketene



Propadienone

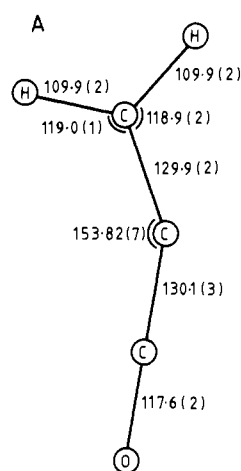


Figure 1. A. Structures derived from B and C rotational constants. Rotational constants used for $\text{D}_2\text{C}_3\text{O}$ were² $B = 3992.03$ (1) and $C = 3830.19$ (1). B. Published structures for formaldehyde¹¹ and ketene.¹² Internuclear distances are given in picometers, and bond angles are in degree.

The out-of-plane methylene bending force constants are reported to be approximately one-third and one-fifth of that for ethylene, respectively.

It is interesting that even very elaborate molecular orbital calculations fail to predict the bent geometry of propadienone, although a low-frequency in-plane bending mode is indicated.⁴

Acknowledgment. This work was supported by a grant from the Australian Research Grant Committee. We are grateful to Dr. Maneerat Woodruff and Dr. Anthony Marchese for preparation of precursors and Dr. Leo Radom for communicating results of his calculations in advance of publication.